PHYSICAL REVIEW B VOLUME 15, NUMBER 1 1 JANUARY 1977

Far-infrared Stark and Zeeman splitting of trivalent rare-earth ions in barium, calcium, and cadmium fluorides

G. Villermain-Lecolier, G. Morlot, P. Strimer, J. P. Aubry, and A. Hadni
University of Nancy I, Nancy, France
(Received 4 November 1975; revised manuscript received 27 May 1976)

We have studied the far-infrared absorption of BaF_2, CaF_2, and CdF_2 doped with Tb, Sm, Nd, Pr, Dy, Ho, Er from room temperature down to 1.4 K. The background absorption induced by the rare-earth (R) impurity is too high in the case of CdF_2 for any electronic transition to be seen. It is low enough for CaF_2- and BaF_2-doped crystals. In the case of all BaF_2:R^{3+} crystals considered, we have found a common absorption band at 131 cm^{-1}. The structure is explained by localized vibrations of the compensation F^- ions, in three different sites: cubic, tetragonal, and trigonal, where the R ions are distributed in different proportions: 4%, 46%, 50%, respectively. We have also found specific bands sensitive to magnetic fields in the case of Dy^{3+} (41.2 cm^{-1}), Ho^{3+} (37 cm^{-1}), and Er^{3+} (69.2 and 70.3 cm^{-1}). The Zeeman effect gives information on the Landé g factors g_1 and g_2 for ground and excited levels, respectively, and shows that for Er^{3+} the observed lines correspond to two different sites. It is shown that $g_1 = g_2 = 3.6$ for the trigonal one and $g_1 = g_2 = 0.98$ for the tetragonal site. For BaF_2:Dy^{3+}, $g_1 = 3.2$, $g_2 < g_1$; for BaF_2:Ho^{3+}, $g_2 - g_1 = 7.6$. In both these crystals only one site (trigonal) has led to far-ir electronic transitions.

INTRODUCTION

Fluoride-type crystals are good hosts for rare-earth (R) ions. Their electronic transitions have been used in several solid-state lasers.[1] There are also many studies of luminescence and absorption spectra in the visible range from room temperature down to 4 K, and also several electron-paramagnetic-resonance (EPR) experiments.[2] Their atomic vibrations have also been studied. Some successful ir studies at around 10 μm on CaF_2 and BaF_2 doped simultaneously with trivalent R ions and H^- ions providing charge compensation (U centers) have been reported.[3] For CaF_2 they show a group of lines around 1300 cm^{-1} due to the interstitial H^-. They are broadened by substitutional H^- which give also a specific absorption at 960 cm^{-1}.

In the low-frequency spectrum, Chase *et al.*[4] have reported the impurity-induced Raman scattering in SrF_2 and BaF_2 doped with Eu^{2+}. The spectra are complicated by large signals from some T_2g modes and some two-phonon scattering. Hayes *et al.*[5] have measured at 1.8 K the far-infrared absorption of CaF_2 doped with Co^{2+}, Y^{3+}, La^{3+}, Sm^{2+}, and Tm^{3+}. A broad absorption has been observed. A simple model incorporating a lattice Green's function, a mass change at the impurity site, and a change of nearest-neighbor central force constant have been used to calculate the ir absorption (activated band modes). There may well be electronic levels of Tm^{3+} in the low-frequency region in addition to the phonon absorption but no sharp line has been observed. More recently Ward *et al.*[6] have studied the far-infrared transmission of CaF_2 doped with erbium.

We intend to show that the comparisons we have made among the series of barium fluoride crystals doped with several R ions, and the study of the Zeeman effect have clarified the problem. It is possible in most cases to separate electronic and vibrational lines.

Some of the vibrational lines are ascribed to local vibrations of the interstitial F^- ions around 131 cm^{-1} similar to the local vibrations of the interstitial H^- ions around 800 cm^{-1}.[3,7,8] From the position of these lines it is possible to infer the symmetry of the corresponding F^--ion site. When electronic lines are found, they can also give an indication of the symmetry at the R-ion site. It is also possible to get an average value of the Landé g factor for both the ground-state and first-excited electronic level of the R ion, and different sites can be found in one crystal.

I. EXPERIMENTAL AND RESULTS

The crystals are grown by the Bridgman-Stockbarger method in a graphite crucible opened in a helium atmosphere.[9] The spectra are recorded with a grating spectrometer.[10]

Figure 1 shows the far-infrared absorption of pure BaF_2 and CaF_2 at 1.4 K. The 146- and 169-cm^{-1} peaks in BaF_2 are ascribed to LA and TO modes at the Brillouin-zone boundary which are made ir active by natural barium isotopes.[11] The 146-cm^{-1} band corresponds to a peak in the density of the phonons observed by neutron scattering at room temperature; the 169-cm^{-1} peak is not

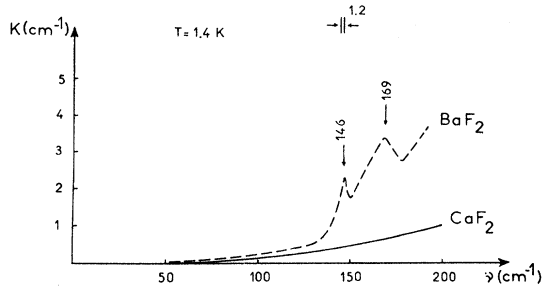

FIG. 1. Absorption coefficient of pure BaF_2 and CaF_2 at 1.4 K.

reported at this temperature.

Figure 2 gives the additional absorption introduced by different R ions: Tb^{3+}, Sm^{3+}, Pr^{3+}, Er^{3+}, Ho^{3+}, and Dy^{3+}. The additional absorption induced by Nd^{3+} is given in Fig. 3. A broad absorption is observed in all spectra with three peaks at 75.5–131.5 and 158 cm^{-1} and either an inflection or a weak band at 125 cm^{-1}.

Sharp lines are seen for Er^{3+} at 69.2 and 70.3 cm^{-1}, for Ho^{3+} at 37 cm^{-1}, and for Dy^{3+} at 41.2 cm^{-1}. A weak absorption is observed at 50.4 cm^{-1} for Ho^{3+}.

The broad absorption band is not modified by a magnetic field and, as it has exactly the same structure for all seven R ions, it may be ascribed either to local vibrations of the common compensation F^- ion or to BaF_2 phonons made ir active by the impurities. Figure 4 shows the additional absorption given by divalent impurities (Co^{2+}–Mn^{2+}–Ni^{2+}) introduced in BaF_2. The spectra have different structures which are now specific to each transition element. We shall explain the 131-cm^{-1}

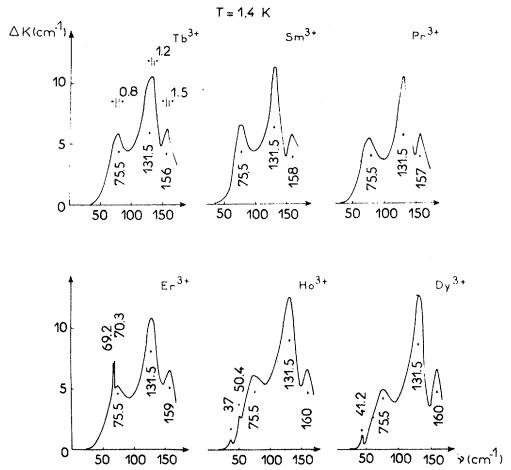

FIG. 2. Additional absorption induced by Tb^{3+}, Sm^{3+}, Pr^{3+}, Er^{3+}, Ho^{3+}, and Dy^{3+} in BaF_2 at 1.4 K from 20 to 170 cm^{-1}.

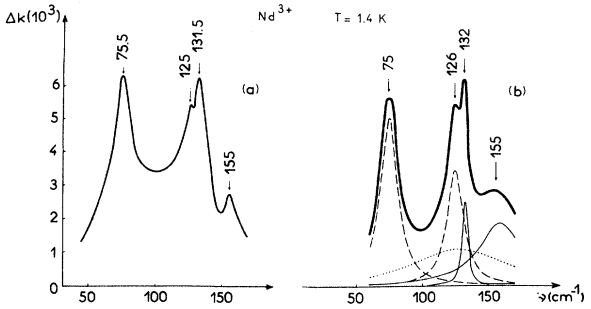

FIG. 3. Additional absorption induced by Nd^{3+} in BaF_2 at 1.4 K from 20 to 170 cm^{-1}. The curve on the left-hand side is the experimental one. On the right-hand side five Lorentz oscillators are considered and the solid curve gives the total computed absorption.

band common to all BaF_2 crystals doped with R in terms of localized vibration of the compensation F^- ion. The specific absorption of divalent impurities will be discussed in another paper.

II. LOCAL MODES OF INTERSTITIAL F^- ION

In the growth conditions described above charge compensation is made by F^- ions and three possible sites are considered: the cubic one where

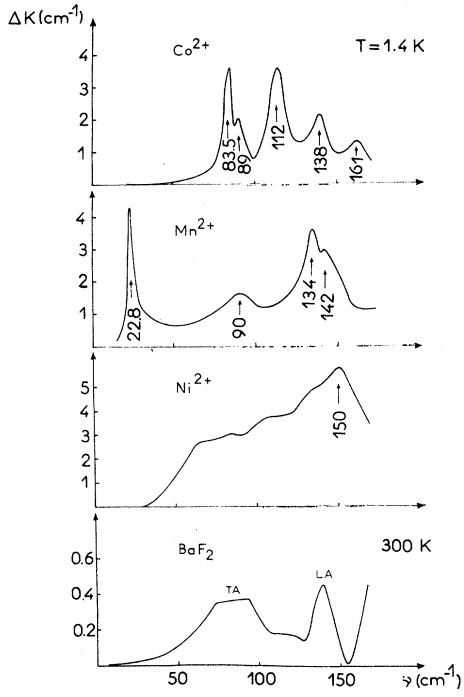

FIG. 4. Additional absorption induced by Co^{2+}, Mn^{2+}, and Ni^{2+} in BaF_2 at. 1.4 K from 20 to 170 cm^{-1}. The lower curve gives the total density of phonons vs ν (from Ref. 18).

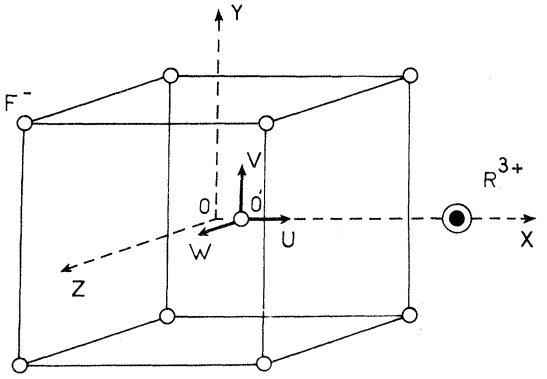

FIG. 5. Structure of CaF_2: R^{3+} in C_{4v} site.

the F^- ion is far from any R ion, the tetragonal site (Fig. 5) where the F^- ion is in the nearest-neighbor (nn) interstitial site at a distance $d \leq \frac{1}{2}a = 3.1$ Å ($a = 6.2$ Å is the lattice constant). The trigonal site (Fig. 6) where the F^- ion is in the second nn interstitial site at a distance of $d' \leq \frac{1}{2}a\sqrt{3} = 5.37$ Å.

The introduction of a fluorine atom for charge compensation gives three additional degrees of freedom for each atom and leads to three vibrational modes. Schäfer was the first to consider a similar problem in 1960.[12] The addition of H^- (U centers) in KCl causes a sharp localized mode at 500 cm^{-1} above the maximum phonon frequency $\nu_M = 205$ cm^{-1}. In the case of alkaline-earth halides H^- localized modes are observed at 1300 and 960 cm^{-1} for CaF_2 and around 800 cm^{-1} for BaF_2. The intuitive argument can be made that such a high-frequency mode, if it involves the impurity at all, must be localized since there are no lattice modes up at this frequency to carry the energy away from the impurity.[13] That is not the case

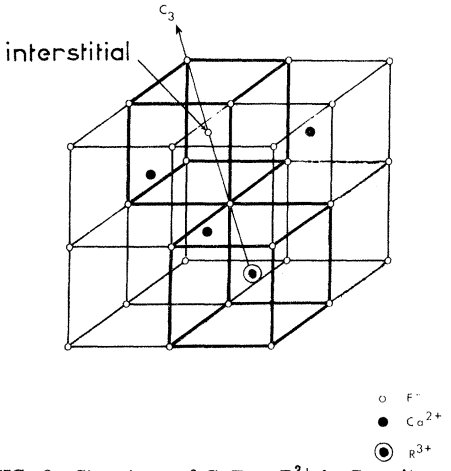

FIG. 6. Structure of CaF_2: R^{3+} in C_{3v} site.

with our problem since the band observed is located in the continuum of acoustic phonons. If the impurity were substitutional a broad response called "resonant mode" should be expected. It is broad not because of damping but because it consists of an envelope of modes, in each of which the defect vibrates with significant enhanced amplitude. However, the impurity is not substitutional but interstitial, located in an empty cubic cell limited by eight fluorine ions. We know that for the interstitial there can be localized modes, gap modes and resonant modes. However very little model fitting has been carried out to date because of the complexity of this defect in the real three-dimensional case.

A. Cubic site

We have thus used a simple model assuming that the F^- compensation ion is surrounded by a rigid lattice including the substitutional R ion. In a cubic site where the F^- ion is far from any R, we shall assume a cubic harmonic potential for the F^- ion of

$$V_1 = \tfrac{1}{2}K(x^2 + y^2 + z^2), \tag{1}$$

(x, y, z) being the components of the fluorine ion displacement.

$$K = m\omega_c^2 \tag{2}$$

is the restoring force constant in the cubic site, m is the mass of the fluorine ion, and ω_c is the oscillation frequency in the cubic site.

B. Lorentz analysis

In Fig. 3 it is clear that the 131-cm^{-1} absorption band is made of at least four components. In fact the cubic site leads to a triply degenerate vibration ω_c, the tetragonal one to a longitudinal singlet ω_L and a doubly degenerate transversal ω_T, and the trigonal site to another longitudinal singlet ω'_L and to another transversal doubly degenerate vibration ω'_T.

We have thus made an analysis of the 131-cm^{-1} experimental band (in the case of $BaF_2:Nd^{3+}$) in terms of five Lorentz oscillators. Their spatial frequencies are labeled ν_L, ν_T, ν'_L, ν'_T, and ν_C in Table I. Each oscillator gives a contribution k_i to the absorption index k, with

$$k_i = \frac{2\pi\rho_i}{n_i}\,\frac{\Omega\delta_i}{(1-\Omega)^2 + \Omega^2\delta_i^2}, \tag{3}$$

where

$$\rho_i = N_i q_i^2/m_i\omega_i^2 \tag{4}$$

is the oscillator strength, N_i the number of type i oscillators, ω_i their angular frequency, $\delta_i = \mu_i/\omega_i$

TABLE I. Analysis of the 131.5-cm^{-1} absorption band in terms of five Lorentz oscillators.

	ν_{expt} (cm^{-1})	ν_i (cm^{-1})	μ_i (cm^{-1})	N_i (cm^{-3})
ν_L	75.5	75	16	1.26×10^{19}
ν_T	155	160	40	
ν'_L	125	125	15	1.35×10^{19}
ν'_T		135	90	
ν_c	131.5	132	5	0.12×10^{19}

their reduced damping constant and $\Omega=\omega/\omega_i$ the reduced frequency at which the absorption is considered; we have taken $q_i=e_0$ (the electric charge of the electron). From Table I we can get the total concentration of Nd^{3+} ions: $N=\sum N_i=2.73\times10^{19}$ ions/cm^3. A radio-activation analysis carried on the same sample has given $N=(2.87\pm0.09)\times10^{19}$ ions/cm^3, which is a first justification of the Lorentz decomposition. For this concentration there are 46% tetragonal sites, 50% trigonal sites and only 4% cubic sites. When the concentration is divided by a factor of 4, we have found an increase on the concentration of cubic sites.

C. Tetragonal site

In the tetragonal site where the compensating fluorine ion is first nn to a R^{3+} ion (Fig. 5) we add a Coulomb potential V_2 due to an excess charge q' at the R^{3+}-ion site. Let us call 0′ the new position of the F^- ion and x_0 the displacement from the cubic position 0 (Fig. 5). In the harmonic approximation we have

$$Kx_0=qq'/4\pi\epsilon_0 d^2, \tag{5}$$

q' being the charge (absolute value) of the compensation fluoride ion and $d=\frac{1}{2}a-x_0$ the distance between the F^- and the R^{3+} ion at equilibrium.

If we consider a small displacement (u,v,w) of the fluorine ion from equilibrium position 0′, we have

$$V_1=\tfrac{1}{2}K[(x_0+u)^2+v^2+w^2],$$

$$V_2=-\frac{1}{4\pi\epsilon_0}\frac{qq'}{[(d-u)^2+v^2+w^2]^{1/2}},$$

and $V=V_1+V_2$. Now for a longitudinal displacement u of the fluorine ion from this tetragonal equilibrium position we can write

$$mu''=-\frac{\partial V}{\partial u}=-K(x_0+u)+\frac{\partial}{\partial u}\left(\frac{1}{4\pi\epsilon_0}\frac{qq'}{(d-u)^2}\right),$$

then

$$mu''\simeq -Kx_0-Ku+\frac{qq'}{4\pi\epsilon_0 d^2}\left(1+\frac{2u}{d}\right),$$

$$mu''\simeq -\left(K-\frac{2qq'}{4\pi\epsilon_0 d^3}\right)u,$$

and

$$\omega_L^2=K/m-2qq'/4\pi\epsilon_0 d^3 m,$$

or

$$\omega_L^2=\omega_c^2-2A, \tag{6}$$

with

$$A=qq'/4\pi\epsilon_0 d^3 m. \tag{7}$$

For a transverse displacement v or w of the fluorine ion from the tetragonal equilibrium position 0′ we are led to a doubly degenerate mode. Newton's law gives

$$mv''=\frac{\partial U}{\partial v}=-Kv+\frac{\partial}{\partial v}\frac{qq'}{4\pi\epsilon_0(d^2+v^2)^{1/2}}$$

or

$$mv''\simeq -Kv-\frac{qq'}{4\pi\epsilon_0}\frac{v}{d^3},$$

hence

$$\omega_T^2=\omega_c^2+A. \tag{8}$$

D. Trigonal site

When the compensation fluorine ion is second nn to a R^{3+} ion, the distance d' between both ions is now larger than d ($d'\simeq d\sqrt{3}$). We have again a longitudinal mode ω'_L and a transversal doubly degenerate one ω'_T:

$$\omega_L'^2=\omega_c^2-2A', \tag{9}$$

$$\omega_T'^2=\omega_c^2+A', \tag{10}$$

with

$$A'=qq'/4\pi\epsilon_0 d'^3 m. \tag{11}$$

A' is smaller than A; ω'_L and ω'_T are much closer to ω_c than ω_L and ω_T.

E. Numerical check

We have ascribed the five Lorentz oscillators to the local modes corresponding to the three different sites of the interstitial fluorine ion considered above; $\nu_c=132$ cm^{-1} (cubic), $\nu_L=75$ cm^{-1} and $\nu_T=160$ cm^{-1} (tetragonal), $\nu'_L=125$ cm^{-1} and $\nu'_T=135$ cm^{-1} (trigonal). From (6) we get $A=2.096\times10^{26}$ rad^2 sec^{-2}; hence $\omega_T^2=\omega_c^2+A$, $\omega_T^2=2.879\times10^{13}$, or $\nu_T=153$ cm^{-1}. The experimental value, 160 $cm^{-1}\pm4$ cm^{-1}, is in good enough agreement. Now, from Eq. (7), $qq'/d^3=4\pi\epsilon_0 mA$, and thus

$$qq'/d^3=7.350\times10^{-10}\ C^2/m^3. \tag{12}$$

On the other hand, from Eq. (2) we get $K=19.54$ N/m. Thus

$$19.54(\tfrac{1}{2}a-d)=qq'/4\pi\epsilon_0 d^2. \tag{13}$$

Combining (12) and (13), we get $d = 2.31$ Å, $x_0 = 0.79$ Å and $(qq')^{1/2} = 0.95 \times 10^{-19}$ C. This value is smaller than the electric charge of the electron ($e_0 = 1.6 \times 10^{-19}$ C). However the agreement is reasonable for the rather crude model which has been considered. The use of an anharmonic potential should lead to higher values of d and qq'. If there should still be some discrepancy it might be due to some screening by the F^- ions.

In the same way using Eq. (9) we get $A' = 3.196 \times 10^{25}$ rad^2 sec^{-2} (trigonal site) and the calculation then gives $\nu'_T = 135$ cm^{-1} in good agreement with the experimental value. We also get $d' = 5.11$ Å, $x'_0 = 0.26$ Å, and $(qq')^{1/2} = 1.22 \times 10^{-19}$ C. The fact that d and d' are, respectively, close to $\frac{1}{2}a$ and $\frac{1}{2}a\sqrt{3} = 5.37$ Å is an additional and important justification of the model.

F. Modification of the 131-cm^{-1} absorption band by hydrogenation

It has been possible to change the structure of the 131-cm^{-1} absorption band of $BaF_2:R^{3+}$ by hydrogenation. A $BaF_2:Nd^{3+}$ crystal (0.2-mole% doping) was heated at 900°C for 24 h in a hydrogen atmosphere (1 atm at 900°C) where PbF_2 and Al were also present at the same temperature.[8] The intensity of the 131-cm^{-1} absorption band is reduced and two new absorption bands appear at 126 and 150 cm^{-1}. These bands had been observed previously[11] after hydrogenation of pure BaF_2, and ascribed, respectively, to a resonant mode of the H^- substitution atoms and to LA phonons made ir active by the substitution H^- ions. The conclusion is that hydrogenation of $BaF_2:Nd^{3+}$ is active to introduce substitution and compensation H^- ion. Irradiation at room temperature (23 h) increases both processes and the sample gets an orange color.

III. ELECTRONIC TRANSITIONS IN $BaF_2:R^{3+}$

The splitting of the R^{3+} ground level by the electric crystal field depends on the R ion site. It is generally accepted that an increase of the lattice cation radius will favor the trigonal site. The compensating F^- ion prefers to occupy the interstitial position along the C_3 axis and does not like to lie along the C_4 axis. For instance, a study of the luminescence spectra of the Dy^{3+} ion in a homologous series of fluorides has shown that in CaF_2 the noncubic centers have tetragonal symmetry; in SrF_2 they are tetragonal and trigonal, while in BaF_2 they are trigonal.[14] We shall see that in the case of $BaF_2:Dy^{3+}$ and $BaF_2:Er^{3+}$ where luminescence studies are available, our far-infrared spectra generally agree with the trigonal energy levels established from these data.

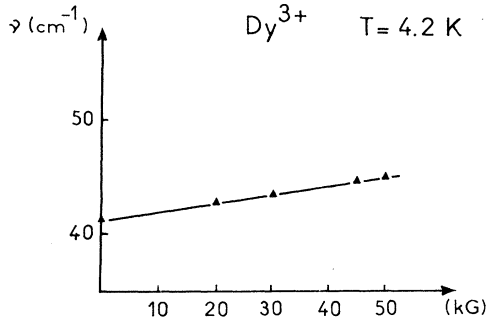

FIG. 7. Zeeman effect for the 41.2-cm^{-1} absorption band of $BaF_2:Dy^{3+}$ which is shifted without evidence of splitting.

A. $BaF_2:Dy^{3+}$

In Fig. 7 we observe a linear shift of the 41.2-cm^{-1} frequency with increasing magnetic field, which shows unambiguously that it arises from an electronic transition. From luminescence spectra, Eremin *et al.*[15] have located three excited levels at 42, 73, and 110 cm^{-1} ascribed to a trigonal site. We have not isolated the absorption lines at 73 and 110 cm^{-1} expected from this scheme. They are located close to maxima in the absorption band ascribed to resonant modes of the compensation F^- ion, and that makes the study more difficult. The ground state of the Dy^{3+} ion is $^6H_{15/2}$. In a crystal field of symmetry lower than the cubic one, it shifts into eight Kramers doublets. This doublet degeneracy is removed by application of a magnetic field H. The lower Kramers doublet gives two components E_1 and E'_1 (Fig. 8);

$$E_1 = -\tfrac{1}{2}g_1\mu_B H, \quad E'_1 = \tfrac{1}{2}g_1\mu_B H.$$

The first excited Kramers doublet gives E_2 and E'_2;

$$E_2 = 41.2 - \tfrac{1}{2}g_2\mu_B H, \quad E'_2 = 41.2 + \tfrac{1}{2}g_2\mu_B H,$$

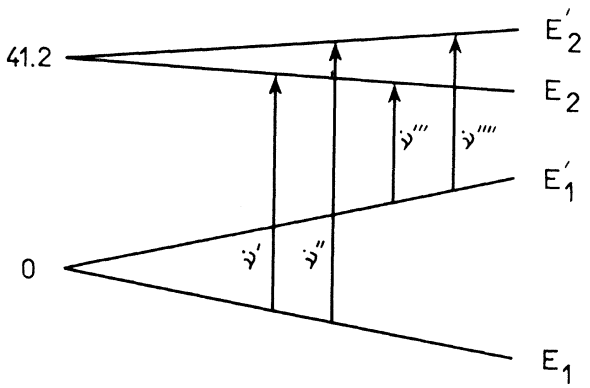

FIG. 8. Kramers doublets splitting in $BaF_2:Dy^{3+}$.

where g_1 and g_2 are, the average Landé g factors of the ground and first excited states, respectively, and $\mu_B = 0.47 \times 10^{-4}$ cm^{-1} G^{-1} is the Bohr magneton. We are thus expecting 4 lines,

$$\nu' = E_2 - E_1 = 41.2 + \tfrac{1}{2}\mu_B H(g_1 - g_2),$$

$$\nu'' = E_2' - E_1 = 41.2 + \tfrac{1}{2}\mu_B H(g_1 + g_2),$$

$$\nu''' = E_2 - E_1' = 41.2 - \tfrac{1}{2}\mu_B H(g_1 + g_2),$$

$$\nu'''' = E_2' - E_1' = 41.2 + \tfrac{1}{2}\mu_B H(g_2 - g_1).$$

In fact, lines ν''' and ν'''' are issued from the E_1' level, which is either experimentally undistinguishable from the E_1 level at low magnetic fields (the spectrometer limit of resolution is 0.8 cm^{-1}), or has too low a population at 1.4 K (1.4 K $\equiv$ 1 cm^{-1}) when high magnetic fields are applied to significantly separate E_1' from E_1. We can only expect lines ν' and ν''. If we assume that lines ν' and ν'' have the same intensity, the position of the experimental absorption maximum will correspond to the center of mass of lines ν' and ν'';

$$\nu_{\text{expt}} = 41.2 + \tfrac{1}{4}\mu_B H(g_1 - g_2 + g_1 + g_2),$$

$$\nu_{\text{expt}} = 41.2 + \tfrac{1}{2}\mu_B g_1 H.$$

In this way, we get $g_1 = 3.2$. We may also note that absorption is negligible for $\nu < 41.2$ cm^{-1} even for the highest magnetic field used, which suggests that $g_2 < g_1$.

B. $BaF_2:Ho^{3+}$

Two characteristic lines are observed at 37 and 50.4 cm^{-1} (Fig. 2). Figure 9 shows a linear shift of the 37-cm^{-1} frequency with an increasing magnetic field, which is a proof of an electronic transition.

In Ho^{3+} there are ten $4f$ electrons and the ground state $^5I_8$ is split into 11 Stark levels by the BaF_2 crystal field. Let us call the two levels involved by the 37-cm^{-1} absorption band E_1 and E_2. The magnetic field will shift both of them;

$$E_1 = \tfrac{1}{2} g_1 \mu_B H,$$

$$E_2 = 37 + \tfrac{1}{2} g_2 \mu_B H;$$

hence

$$\nu = 37 + \tfrac{1}{2}\mu_B H(g_2 - g_1),$$

and $g_2 - g_1 = 7.6$.

The 50.4-cm^{-1} line is not sensitive to magnetic fields in the range of the experiment ($H \leq 50$ kG).

C. $BaF_2:Er^{3+}$

Two electronic lines are observed at $\nu_1 = 69.2$ and $\nu_2 = 70.3$ cm^{-1} in good agreement with luminescence data interpreted in the assumption of a trigonal site.[16] Each one is split into a doublet when a magnetic field is applied (Fig. 10).

From the above discussion related to $BaF_2:Dy^{3+}$ we shall ascribe its two components to ν' and ν''. We thus have, (i) for the $\nu_1 = 69.2$ cm^{-1} electronic band;

$$\nu_1' = 69.2 + \tfrac{1}{2}\mu_B H(g_1 - g_2), \quad \nu_1'' = 69.2 + \tfrac{1}{2}\mu_B H(g_1 + g_2).$$

Now, frequency ν_1' being independent of magnetic field H, we can write $g_1 \simeq g_2 \simeq 3.6$. (ii) for the $\nu_2 = 70.3$ cm^{-1} electronic band;

$$\nu_2' = 70.3 + \tfrac{1}{2}\mu_B H(g_1 - g_2), \quad \nu_2'' = 70.3 + \tfrac{1}{2}\mu_B H(g_1 + g_2).$$

Here again frequency ν_2' is independent of H and $g_1 = g_2 \simeq 0.98$.

The conclusion is that the ground state from which each electronic line at 69.2 and 70.3 cm^{-1} originates has quite different g_1 values. They correspond to Er^{3+} ions in two different sites where the Landé factors g_1 are different. They could correspond to one trigonal site and one tetragonal site. However, the EPR measurements of Antipin *et al.*, $g_1 = 6.734$ for trigonal sites and $g_1 = 6.755 \pm 0.02$ for cubic sites,[2] are quite different.

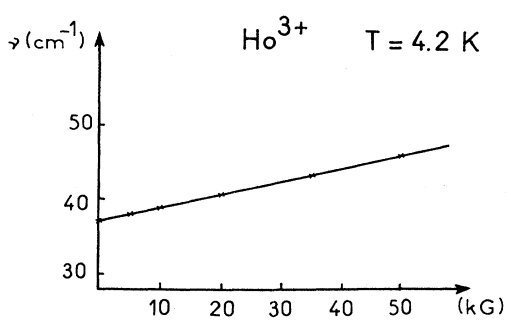

FIG. 9. Zeeman effect observed at 4.2 K for the ν_1 electronic line of Ho^{3+} ($\nu_1 = 37$ cm^{-1}) in BaF_2, which is shifted without splitting.

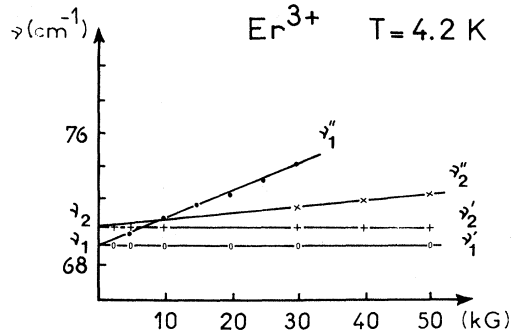

FIG. 10. Zeeman effect observed at 4.2 K for the ν_1 and ν_2 electronic lines of Er^{3+} ($\nu_1 = (69.2$ cm^{-1}; $\nu_2 = 70.3$ cm^{-1}) in BaF_2, which split into two doublets.

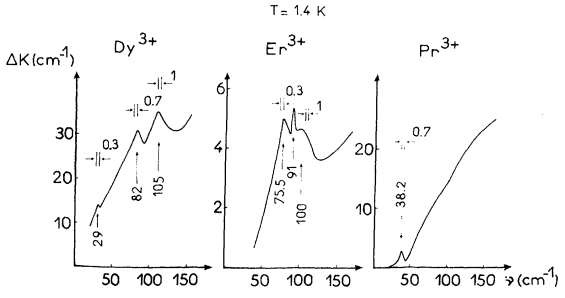

FIG. 11. Additional absorption induced by Er^{3+}, Dy^{3+}, and Pr^{3+} in CaF_2 at 1.4 K from 20 to 170 cm^{-1}.

IV. CASE OF CaF_2 DOPED WITH R^{3+} IONS

A. $CaF_2:R^{3+}$

In Fig. 11 the central curve corresponds to a 0.2-mole% ErF_3 doping in the crucible and it is the only one which can be compared to the above spectra concerning BaF_2 because the doping is the same. The induced absorption has the same order of magnitude as in Fig. 2 concerning BaF_2, and agrees with the work of Ward *et al.*[6]

They have described two electronic lines at 21.10 and 32.76 cm^{-1} in $CaF_2:Er^{3+}$ and explained them on the assumption of a tetragonal site. This should be in good accordance with Stolov who has shown that tetragonal and cubic sites were predominant in $CaF_2:R^{3+}$ while trigonal ones were more abundant in $BaF_2:R^{3+}$.

The curves concerning $CaF_2:Dy^{3+}$ and $CaF_2:Pr^{3+}$ correspond to a higher doping (1%) and the background absorption is higher.

B. $CdF_2:R^{3+}$

In that case the background-induced absorption is much higher than in the case of doped CaF_2 or BaF_2, and it is impossible to see any electronic transition. This might be linked to the fact that the radius of the Cd^{2+} ion is the smallest of the three (0.89 Å), and also the CdF_2 cell parameter (5.38 Å). On the contrary, in the case of BaF_2 there is a good match both for the atomic masses and the ionic radius when R ions are substituted to Ba^{2+}.

V. CONCLUSIONS

The electronic level at 37 cm^{-1} in $BaF_2:Ho^{3+}$ is a new one. On the other hand for $BaF_2:Dy^{3+}$ Eremin *et al.*[15] found a level at 42 cm^{-1} close to the 41.2-cm^{-1} line we observed. For $BaF_2:Er^{3+}$ Aizenberg *et al.*[16] found levels at 70, 76, 80, and 88 cm^{-1} ascribed to a trigonal site, while Zverev *et al.*[17] located a level at 70 cm^{-1} from EPR experiments on a tetragonal site. In fact for $BaF_2:Er^{3+}$ we observed two lines close to 70 cm^{-1} with two different g_1 factors for the ground sublevel from which the 69.2- and 70.3-cm^{-1} lines originate. This shows that we have two types of Er^{3+} sites. One may be trigonal and the other one tetragonal since the resonant modes have shown these types of sites were the most important. This explanation agrees with the work of Aizenburg *et al.* and with that of Zverev and Smirnov.

ACKNOWLEDGMENTS

The authors are grateful to Dr. R. Mellet of the Centre National Etudes des Télécommunications (Bagneux, France) for the radio-activation analysis of the doped crystals.

[1]Z. J. Kiss and R. C. Duncan, Proc. IRE 50, 1531 (1962).
[2]A. A. Antipin, I. N. Kirkin, L. D. Kivanova, L. Z. Portvorova, and L. Ya. Shekun, Sov. Phys.-Solid State 8, 2130 (1967).
[3]G. D. Jones and R. A. Satten, Phys. Rev. 147, 566 (1966).
[4]L. L. Chase, D. Kuhner, and W. E. Bron, Phys. Rev. B 7, 3892 (1973).
[5]W. Hayes, M. C. K. Wiltshire, R. Bernhman, and P. R. W. Hudson, J. Phys. C 6, 1157 (1973).
[6]R. W. Ward and B. P. Clayman, J. Phys. C 7, L322 (1974); and 8, 872 (1975).
[7]J. A. Harrington, R. T. Harley, and C. T. Walker, Solid State Commun. 8, 407 (1970).
[8]R. J. Elliott, W. Hayes, D. G. Jones, N. F. MacDonald, and C. P. Sennet, Proc. R. Soc. Lond. A 289, 1 (1965).
[9]I. V. Stepanov and P. P. Feofilov, in *Growth of Crystals*, edited by A. V. Shubnikov and N. N. Sheftal (Consultants Bureau, New York, 1959), Vol. 2.
[10]A. Hadni and P. Strimer, Phys. Rev. B 5, 4609 (1972).
[11]J. A. Harrington and R. Weber, Phys. Status Solidi B 56, 541 (1973).
[12]G. Schafer, J. Phys. Chem. Solids 12, 233 (1960).
[13]A. S. Barker and A. J. Sievers, Rev. Mod. Phys. 47, (No. 2), (1975).
[14]N. S. Al'tshuler, M. V. Eremin, R. K. Luks, and A. L. Stolov, Fiz. Tverd. Tela 11, 3484 (1969).
[15]M. V. Eremin, R. K. Luks, and A. L. Stolov, Fiz. Tverd. Tela 12, 3473 (1970).
[16]J. B. Aizenberg, L. D. Livanova, J. G. Saitkulov, and A. L. Stolov, Fiz. Tverd. Tela 10, 2030 (1968).
[17]G. M. Zverev and A. I. Smirnov, Fiz. Tverd. Tela 6, 96 (1964).
[18]J. P. Hurrell and V. J. Minkiewicz, Solid State Commun. 8, 463 (1970).